J. Fluid Mech. (1987), *vol.* 179, *pp.* 469–487
Printed in Great Britain

Triple-deck solutions for supersonic flows past flared cylinders

By PH. GITTLER AND A. KLUWICK

Institut für Strömungslehre und Wärmeübertragung, Technische Universität Wien, Wiedner Hauptstraße 7, A-1040 Wien, Austria

(Received 3 December 1985 and in revised form 27 October 1986)

Using the method of matched asymptotic expansions, the interaction between axisymmetric laminar boundary layers and supersonic external flows is investigated in the limit of large Reynolds numbers. Numerical solutions to the interaction equations are presented for flare angles α that are moderately large. If $\alpha > 0$ the boundary layer separates upstream of the corner and the formation of a plateau structure similar to the two-dimensional case is observed. In contrast to the case of planar flow, however, separation can occur also if $\alpha < 0$, owing to the axisymmetric effect of overexpansion and recompression. The separation point then is located downstream of the corner and, most remarkable, a hysteresis phenomenon is observed.

1. Introduction

One of the goals of interacting-boundary-layer theory is to contribute to the understanding of the high-Reynolds-number flow around three-dimensional bodies. In view of the complexity of such flows which is present even in the classical (hierarchical) approach it is, however, not surprising that results have been obtained so far only for a rather limited number of cases. As a first step triple-deck equations for subsonic flow over a three-dimensional hump on a flat plate have been formulated by Smith, Sykes & Brighton (1977). Owing to the complicated form of the pressure-displacement relationship, only solutions to the linearized version of these equations could be calculated. Solutions of the nonlinear interaction equations have been obtained just recently by Duck & Burggraf (1986). (Earlier nonlinear results by Sykes (1978), (1980) were based on a simplified version of the pressure-displacement relationship which is of relevance if stratification effects are of importance outside the boundary layer.)

Nonlinear three-dimensional interaction effects can be studied more easily and in greater detail if it is possible to exploit symmetry properties. Such simplifications include swept-wing configurations and axisymmetric bodies. The case of supersonic flow over a swept compression ramp was investigated first by Vatsa & Werle (1977) and Werle, Vatsa & Bertke (1973), using their interacting-boundary-layer model and by Gittler (1984, 1985), Kluwick (1987) on the basis of triple-deck theory. Since the flow in the lower deck is incompressible to leading order the equations which govern the flow in the directions perpendicular and tangential to the corner are decoupled, which considerably simplifies the numerical computations compared to Vatsa & Werle (1977). As a consequence it was also found possible to treat configurations with geometry varying slowly in the spanwise direction (Gittler 1985; Kluwick 1987).

In the axisymmetric case the cross-flow component vanishes identically and the

description of the flow field only differs from the two-dimensional counterpart because of the more complicated form of the pressure-displacement relationship, provided the boundary-layer thickness is small compared to the characteristic diameter of the body. For supersonic free-stream Mach numbers this relationship then reduces to the result derived by Lighthill (1945) and Ward (1948) in their studies of inviscid quasi-cylindrical flow. According to this theory the flow over an axisymmetric compression (expansion) ramp leads to the phenomenon of overcompression (overexpansion), e.g. the pressure distribution starts with a jump discontinuity of strength $O(\alpha)$ and then gradually decreases (increases) to level of $O(\alpha^2)$ where α denotes the scaled turning angle. One effect of viscosity is to reduce the pressure peak and it is therefore to be expected that incipient separation on an axisymmetrical ramp will occur at larger values of the turning angle than in the two-dimensional counterpart. As was shown by Kluwick, Gittler & Bodonyi (1984), henceforth denoted as I, this is indeed the case. However, since converged solutions could be obtained for moderate values of $|\alpha|$ only two basic questions which arise in connection with axisymmetric ramp flow remained unanswered.

Axisymmetric compression ramps were studied first by Horton (1971) and Vatsa & Werle (1977), and using the triple-deck concept by Duck (1984) and in I. As is well known from the studies of plane flow a plateau region develops upstream of the corner if α is sufficiently large (Rizzetta, Burggraf & Jenson 1978; Ruban 1978). Recently the asymptotic properties of an axisymmetric compressive free interaction solution in which the pressure approaches a constant value far downstream were derived by Kluwick, Gittler & Bodonyi (1985). It is thus of interest to investigate whether this self-similar solution is of relevance for axisymmetric ramp flows.

If the turning angle is negative the flow initially accelerates but owing to the phenomenon of overexpansion the pressure downstream of the corner eventually has to rise again. Accordingly, the skin-friction distributions calculated in I exhibit a maximum upstream of the corner and a minimum downstream of it. As shown in I the minimum value of the skin friction initially decreases with increasing values of $|\alpha|$. Therefore, the possibility that the boundary layer separates downstream of the corner if $-\alpha$ is sufficiently large cannot be ruled out. This is in contrast to the case of two-dimensional supersonic flow over an expansion ramp studied by Matveeva & Neiland (1967), Stewartson (1970*b*) and Rizzetta *et al.* (1978) where the pressure decreases monotonically throughout the interaction region. If the free-stream Mach number is subsonic, however, a recompression of the medium also takes place in the two-dimensional case and the occurrence of separation at large turning angles has recently been demonstrated by Smith & Merkin (1982).

While the separation process upstream of a plane or axisymmetric compression ramp is self-induced the decrease of the skin friction downstream of an axisymmetrical expansion ramp is caused by a pressure increase which is already present if viscous effects are neglected. In this respect the problem considered here bears some similarity with the properties of incompressible flow over a thin airfoil at incidence if the leading edge is rounded such as to force incipient separation to occur there rather than at the trailing edge as has been studied numerically by Ermak (1969) and Werle & Davies (1972). As pointed out by Ruban (1981*b*) the solution of classical boundary-layer theory at incipient separation then has the remarkable property that it can be extended continuously through the point of vanishing skin friction. It is interesting to note that this solution is closely related to the results of Oswatitsch (1957) in his study of boundary-layer separation. In contrast to the case investigated by Stewartson (1970*a*), therefore, the singularity which develops at the separation

point according to the classical hierarchical approach is weak provided the angle of attack differs only slightly from the value at incipient separation, and an interactive theory may be used to obtain uniformly valid solutions (Ruban 1981*a*; Stewartson, Smith & Kaups 1982; Brown & Stewartson 1983). Most interesting, it is found that there is a range of values of the angle of attack for which these solutions are not unique. This leads to the question of whether a similar phenomenon may occur also in the case of supersonic flow over an axisymmetric expansion ramp.

2. Problem formulation

The following study is concerned with the properties of viscous flow over flared cylinders, as depicted in figure 1, at high values of the Renolds number $Re = \tilde{u}_\infty \tilde{L}/\tilde{\nu}_\infty$. Here $\tilde{u}_\infty$, $\tilde{L}$ and $\tilde{\nu}_\infty$ respectively denote the free-stream velocity, the distance of the corner from the front of the cylinder and the kinematic viscosity in the external stream. It will be assumed that the boundary layer that forms on the cylindrical body of radius $\tilde{a} = O(Re^{-\frac{3}{8}}\tilde{L})$ is laminar and that the external flow is supersonic. Asymptotic analysis for

$$\epsilon = Re^{-\frac{1}{8}} \ll 1 \tag{1}$$

then shows that the region in which the interaction between the laminar boundary layer and the inviscid outer flow takes place exhibits a three-layered structure now commonly termed triple-deck structure. As in the two-dimensional counterpart of the problem considered here (Rizzetta *et al.* 1978), the properties of the upper deck and main deck may be investigated analytically while the solution of the lower-deck equations in general requires numerical treatment. For simplicity in the numerical computations it is convenient to scale as many of the physical parameters as possible out of these equations. To this end the following scaled variables are introduced (see I):

$$\left.\begin{aligned}
x &= C^{-\frac{3}{8}}\lambda^{\frac{1}{4}}|M_\infty^2-1|^{\frac{3}{8}}\left(\frac{\tilde{T}_w}{\tilde{T}_\infty}\right)^{-\frac{3}{2}}\frac{\tilde{x}-\tilde{L}}{\epsilon^3\tilde{L}},\\
y &= C^{-\frac{1}{8}}\lambda^{\frac{3}{4}}|M_\infty^2-1|^{\frac{1}{8}}\left(\frac{\tilde{T}_w}{\tilde{T}_\infty}\right)^{-\frac{3}{2}}\frac{\tilde{r}-\tilde{a}}{\epsilon^5\tilde{L}},\\
p &= C^{-1}\lambda^{-\frac{1}{2}}|M_\infty^2-1|^{\frac{1}{4}}\frac{\tilde{p}-\tilde{p}_\infty}{\epsilon^2\tilde{\rho}_\infty\tilde{u}_\infty^2},\\
u &= C^{-\frac{1}{8}}\lambda^{-\frac{1}{4}}|M_\infty^2-1|^{\frac{1}{8}}\left(\frac{\tilde{T}_w}{\tilde{T}_\infty}\right)^{-\frac{1}{2}}\frac{\tilde{u}}{\epsilon\tilde{u}_\infty},\\
v &= C^{-\frac{3}{8}}\lambda^{-\frac{3}{4}}|M_\infty^2-1|^{-\frac{1}{8}}\left(\frac{\tilde{T}_w}{\tilde{T}_\infty}\right)^{-\frac{1}{2}}\frac{\tilde{v}}{\epsilon^3\tilde{u}_\infty},\\
A &= C^{-\frac{1}{8}}\lambda^{\frac{3}{4}}|M_\infty^2-1|^{\frac{1}{8}}\left(\frac{\tilde{T}_w}{\tilde{T}_\infty}\right)^{-\frac{3}{2}}\frac{\tilde{A}}{\epsilon^5\tilde{L}},\\
a &= C^{-\frac{3}{8}}\lambda^{\frac{5}{4}}|M_\infty^2-1|^{\frac{7}{8}}\left(\frac{\tilde{T}_w}{\tilde{T}_\infty}\right)^{-\frac{3}{2}}\frac{\tilde{a}}{\epsilon^3\tilde{L}},
\end{aligned}\right\} \tag{2}$$

where $\tilde{p}$, $\tilde{\rho}$, $\tilde{T}$, $\tilde{x}$, $\tilde{r}$, $\tilde{u}$, $\tilde{v}$, $\tilde{A}$, M and C respectively denote the pressure, the density, the temperature, the streamwise and radial coordinates, the axial and radial velocity

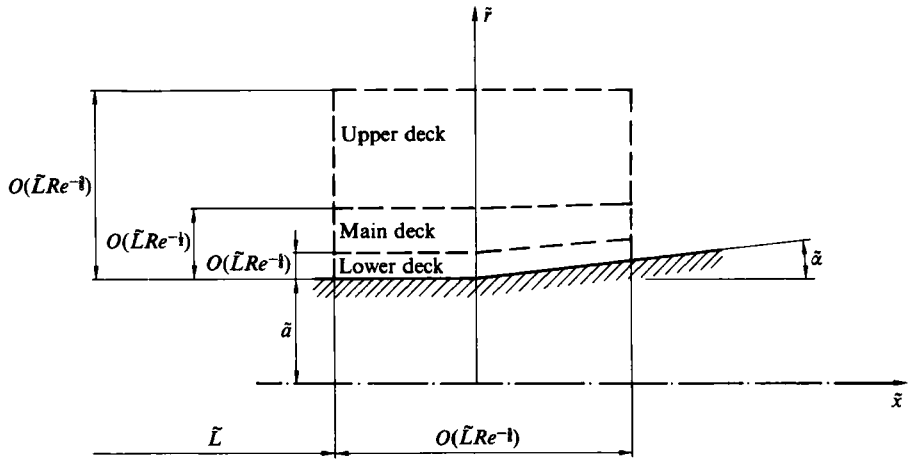

FIGURE 1. Triple-deck structure of the interaction region.

components, the disturbance of the displacement thickness, the Mach number, and the Chapman constant occurring in the linear viscosity law

$$\frac{\tilde{\mu}}{\tilde{\mu}_\infty} = C\frac{\tilde{T}}{\tilde{T}_\infty},$$

while indices ∞ and w refer to free-stream and wall conditions, respectively. Furthermore, $\lambda = 0.33206$ just as in the planar case.

Using the above definitions, the governing equations in the lower deck, to leading order, reduce to

$$\left.\begin{aligned} u\frac{\partial u}{\partial x}+v\frac{\partial u}{\partial y} &= -\frac{\mathrm{d}p}{\mathrm{d}x}+\frac{\partial^2 u}{\partial y^2}, \quad \frac{\partial u}{\partial x}+\frac{\partial v}{\partial y}=0, \\ u &= v = 0 \quad \text{for } y = F(x), \\ u &= y+A(x), \quad y\to\infty \quad \text{for all } x, \\ u &= y, \quad x\to-\infty \quad \text{for all } y, \\ p(x) &= -A'(x)+\frac{1}{a}\int_{-\infty}^{x} W\left(\frac{x-\xi}{a}\right)A'(\xi)\,\mathrm{d}\xi. \end{aligned}\right\} \tag{3}$$

Here

$$W(z) = \int_0^\infty \frac{\mathrm{e}^{-\lambda z}}{K_1^2(\lambda)+\pi^2 I_1^2(\lambda)}\frac{\mathrm{d}\lambda}{\lambda}$$

denotes the function introduced by Ward (1948) in his study of quasi-cylindrical flow and $y = F(x)$ characterizes the body shape. In the case considered here

$$F(x) = \begin{cases} 0, & x < -\rho, \\ \alpha\left[\dfrac{x^2}{4\rho}+\dfrac{x}{2}+\dfrac{\rho}{4}\right], & -\rho \leqslant x \leqslant \rho, \\ \alpha x, & x > \rho, \end{cases} \tag{4}$$

which corresponds to the smoothed version of the cylinder–cone problem investigated

in I. The case of a sharp corner is obtained in the limit $\rho = 0$. Furthermore, the values α and $\tilde{\alpha}$ of the scaled and unscaled ramp angle are related by

$$\alpha = C^{-\frac{1}{4}}\lambda^{-\frac{1}{2}}|M_\infty^2 - 1|^{-\frac{1}{4}}\frac{\tilde{\alpha}}{\epsilon^2}. \tag{5}$$

Finally, by applying Prandtl's transposition theorem (e.g. Rosenhead 1963)

$$z = y - F(x), \quad w = v - uF'(x) \tag{6}$$

the boundary-value problem (3) is written in the form

$$u\frac{\partial u}{\partial x} + w\frac{\partial u}{\partial z} = -\frac{\mathrm{d}p}{\mathrm{d}x} + \frac{\partial^2 u}{\partial z^2}, \quad \frac{\partial u}{\partial x} + \frac{\partial w}{\partial z} = 0, \tag{7a, b}$$

$$u = w = 0 \quad \text{at } z = 0 \tag{7c}$$

$$u \to z + A(x) + F(x), \quad z \to \infty, \quad \text{for all } x, \tag{7d}$$

$$u \to z, \quad x \to -\infty, \quad \text{for all } z, \tag{7e}$$

$$p(x) = -A'(x) + \frac{1}{a}\int_{-\infty}^{x} W\left(\frac{x-\xi}{a}\right)A'(\xi)\,\mathrm{d}\xi, \tag{7f}$$

which will be used in the subsequent sections.

3. Numerical method

The system of equations and boundary conditions (7) was cast into finite-difference form using centred differences in the normal direction and the implicit Crank–Nicolson scheme of second order for the streamwise direction. The numerical method closely follows that of Brown & Williams (1975). The only difference concerns the relationship (7*f*) between $p(x)$ and $A(x)$ in which the function $W(z)$ was determined by means of Gauss–Laguerre formula (cf. Kluwick *et al.* 1985).

Exploiting the parabolic nature of the problem, the numerical solution is initiated at a suitably chosen negative value of x, x_1 say, by giving the pressure a small increment p_1 and taking the velocity profile to be that of a uniform shear flow. The solution of the problem for $x < 0$ then develops in one of three different ways, according to whether p_1 is positive, negative or zero. If p_1 is zero, the trivial solution $u = y, v = 0, p = 0$ is obtained, whereas a positive or negative pressure kick results in the formation of a compressive or expansive free interaction, respectively (Kluwick *et al.* 1985). Far downstream of the corner it is required that the pressure distribution exhibits the asymptotic behaviour

$$p \sim \alpha\left[\frac{a}{x} + 2\frac{a^3}{x^3}\ln\frac{x}{a} + O\left(\frac{a^3}{x^3}\right)\right] \tag{8}$$

following from inviscid theory. We can then expect a unique solution in which the pressure at x_1 is a fixed value p_1. As in the investigations of Daniels (1974) the value of p_1 was held fixed at $+10^{-6}, (-10^{-6})$ for $\alpha > 0, (\alpha < 0)$, respectively, and x_1 was adjusted since this procedure avoids the iterative repetition of the computations in $x < -\rho$.

As already pointed out, the solution for $p_1 \neq 0$ takes on one of two distinct forms, terminating either in a singularity ($x_1 = x_A, p \to -\infty, \tau \to +\infty, x \to x_s$) or in a plateau structure ($x_1 = x_B, p \to \text{const.}, \tau \to 0-, x \to \infty$). Taking a new value $x_1 = \frac{1}{2}(x_A + x_B)$ the

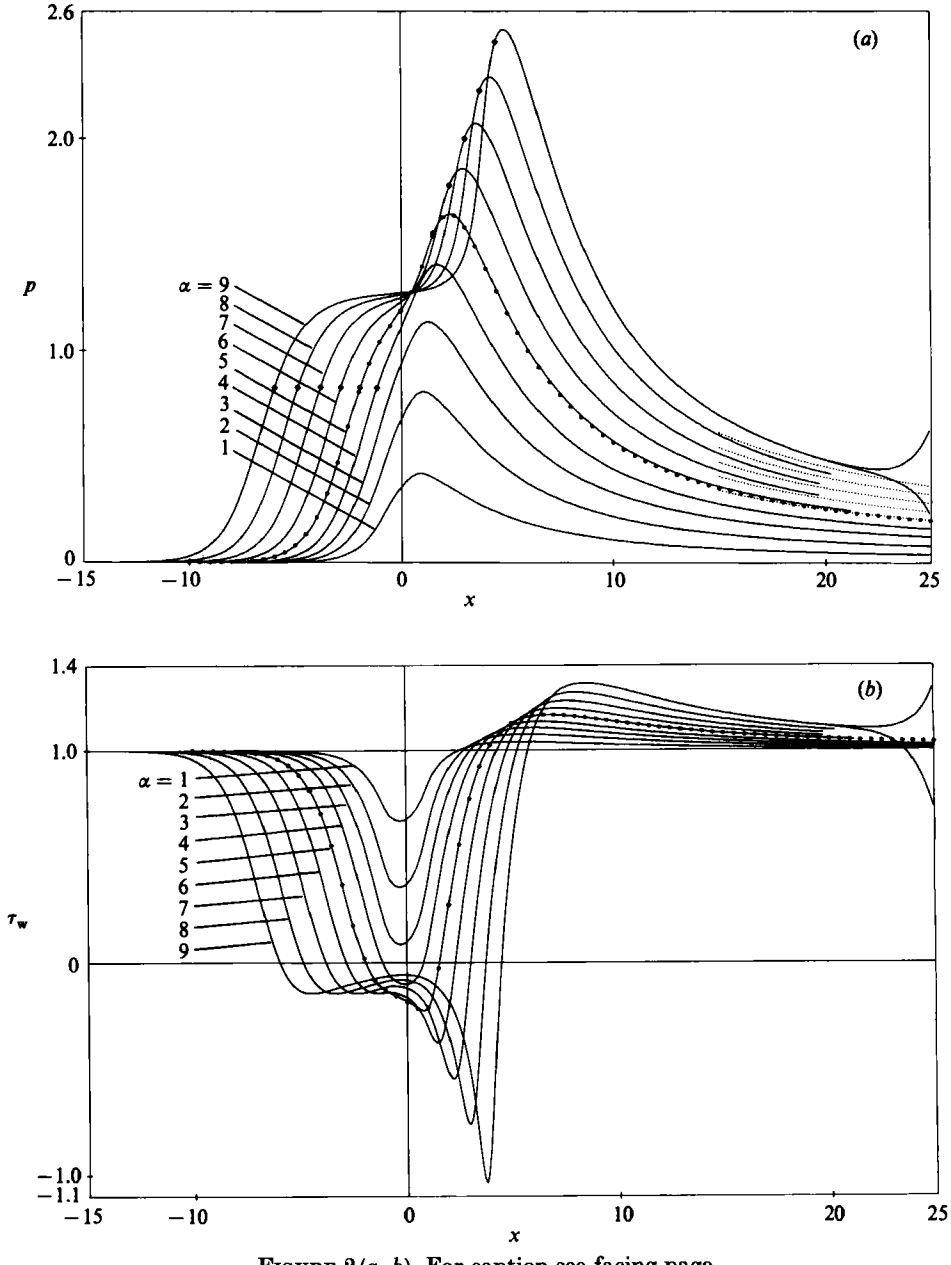

FIGURE 2 (*a*, *b*). For caption see facing page.

solution was computed again, x_1 readjusted accordingly and the process repeated until the difference between the old and the new value was less than 10^{-12}. In this way x_1 converges to a value of highest possible accuracy ($\approx$ 15 digits, depending on the machine error) which ensures that the undesirable occurrence of an expansive or compressive eigensolution is pushed downstream as far as possible.

All numerical results are shown in x-sections in which the difference between the expansive and the compressive solution is less than the plotting accuracy. The

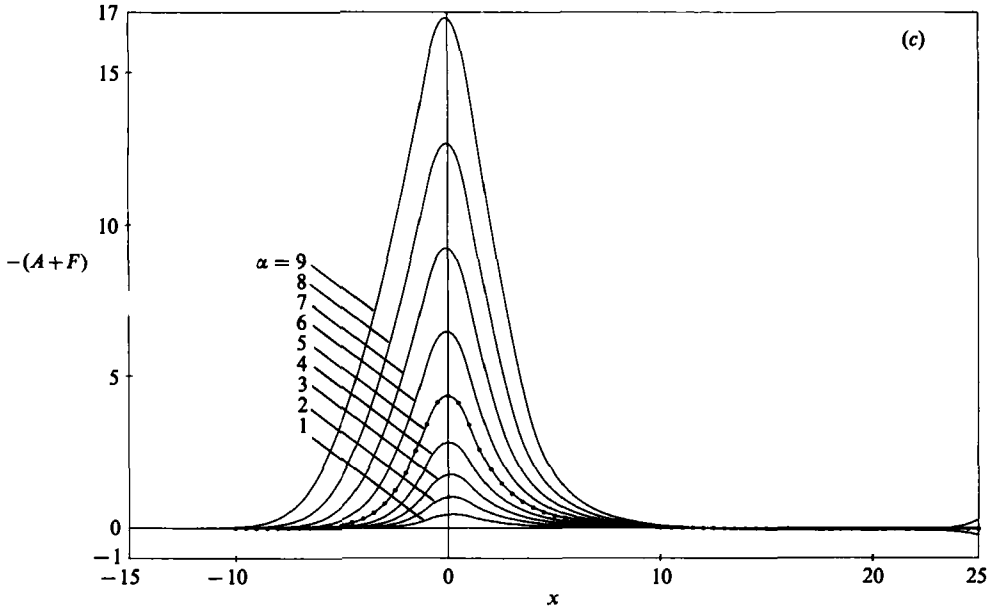

FIGURE 2. Numerical results for $a = 1, \rho = 1$ and various positive cone angles α: ——, $\alpha = 1$–4; and oooo, $\alpha = 5$, spectral method according to I, $N_x = 400$, $\Delta x = 0.25$–0.5, $N_z = 40$, $\Delta z = 0.3$; ——, $\alpha = 5$–9, finite-difference method, $\Delta x = 0.05$, $\Delta z = 0.2$. (*a*) Pressure distribution $p(x)$: ·····, asymptotic relationship (8); ◇, separation and reattachment points. (*b*) Wall-shear-stress distribution $\tau_w(x)$. (*c*) Displacement thickness distribution $-A(x)$.

divergent behaviour of the two eigensolutions for $x \to \infty$ is shown only in figure 2 for $\alpha = 9$ and figure 4 for $\alpha = -11.5$.

Since the equations of motion are parabolic in the streamwise direction, a difficulty arises if recirculation zones exist in the flow field. As in many previous investigations of separated boundary layers (for example Smith 1977) the Reyhner & Flügge-Lotz (1968) approximation was used to prevent numerical instability once flow reversal occurs. Provided the reversed mass flux is not too large, this approximation should give a fairly accurate solution. This is confirmed by the very good agreement between the calculated pressure distribution and the asymptotic relationship (8) – even for large values of $|\alpha|$ – since the numerical program, outlined above, works automatically and leads to a unique solution whose behaviour for $x \to \infty$ cannot be influenced, in contrast to the spectral method used in I.

4. Results for positive cone angles

Before turning to the more interesting case $\alpha < 0$ we briefly summarize the results for positive cone angles. Figure 2(*a*) shows the pressure distribution inside the interaction region for $a = 1, \rho = 1$ and various values of $\alpha > 0$. For comparison the results for $\alpha \leqslant 5$, which were obtained earlier in I by means of a spectral method, are also included herein. As can be seen, both results for $\alpha = 5$ are in excellent agreement over most of the interaction region. Minor discrepancies which occur for large x most probably reflect the inability of the spectral solution to satisfy the asymptotic relationship (8) owing to its inherently periodic structure.

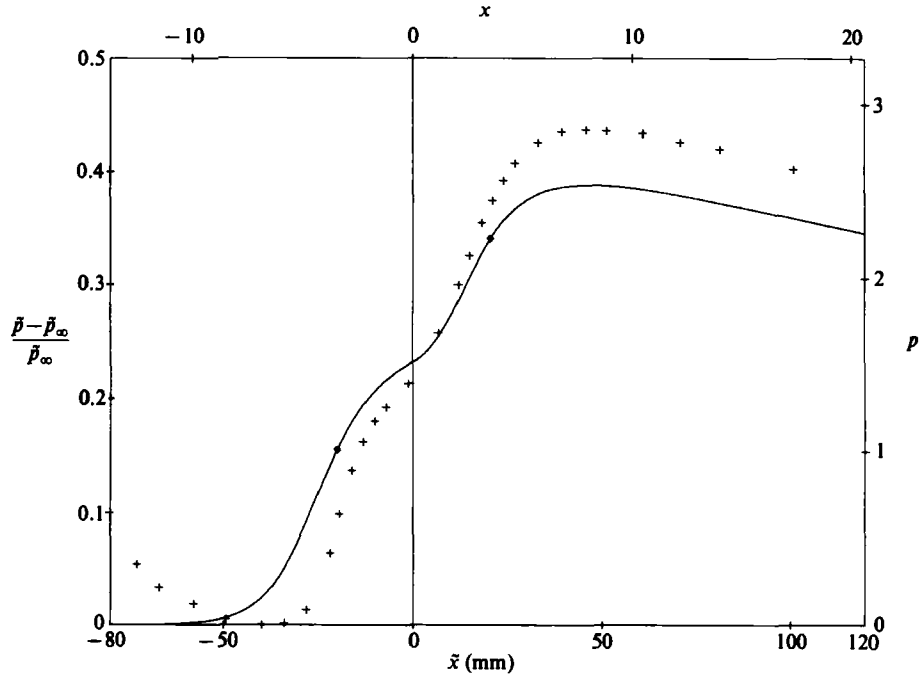

FIGURE 3. Comparison between experimental and theoretical results: + + + +, experimental data from Leblanc & Ginoux (1970, figure 4*a*); $M_\infty = 2.25$, $Re = 8.7 \times 10^4$, $\tilde{\alpha} = 7.5°$, $a = 34.6$; ——, present calculations, finite-difference method, $\Delta x = 0.05$, $\Delta z = 0.2$; ◇, separation and reattachment point.

As expected, the pressure increase due to reattachment is much smaller than in the two-dimensional case. Moreover, the maximum of the pressure distribution differs only slightly from the value at the reattachment point and the compression region upstream of the reattachment point is followed by a zone of rapid expansion caused by the increasing stream tube area. Finally, it should be noted that the formation of a plateau region for large values of α is clearly visible in figure 2(*a*).

As shown by Kluwick *et al.* (1985) the behaviour of $A(x)$ inside the plateau region is given by

$$A(x) \sim -\frac{p_0 x^2}{2a \ln x}\left[1+\frac{2}{\ln x}\left(\frac{3}{4}-\frac{1}{2}\ln\frac{2}{a}\right)\right]. \tag{9}$$

In order to estimate the length L_{sep} of the separated flow region for α large we tacitly assume (i) that the length of the zone over which reattachment is (almost) completed is small compared to the interaction lengthscale, as in the two-dimensional case studied by Daniels (1979, 1980), so that axisymmetric effects are negligibly small; and (ii) that the pressure increase at reattachment is equal to the stagnation pressure of the reattachment streamline (Messiter, Hough & Feo 1973; Burggraf 1975). Using (9) and the result derived by Kluwick *et al.* (1985) that the structure of the free shear layer in the plateau region is just the same as in the case of planar flow (Stewartson & Williams 1973) one then obtains

$$\alpha - \frac{p_0 L_{\text{sep}}}{a \ln L_{\text{sep}}} - C^{-\frac{1}{3}} L_{\text{sep}}^{\frac{2}{3}} = o(\alpha), \tag{10}$$

where $C \approx 3.47$ (Burggraf 1975).

Since $L_{sep}^{\frac{3}{2}} = o(L_{sep}/\ln L_{sep})$ and $p_0 = O(1)$ (Kluwick *et al.* 1985), (10) reduces to

$$\alpha = O\left(\frac{p_0 L_{sep}}{a \ln L_{sep}}\right). \tag{11}$$

Thus the length of the recirculation zone forming on a flared cylinder is much smaller than that caused by a two-dimensional compression ramp of equal turning angle α, where one finds $L_{sep} = O(\alpha^{\frac{3}{2}})$ (Burggraf 1975). As a consequence, also the pressure rise Δp_r due to reattachment is smaller, although $\Delta p_r = O(L_{sep}^{\frac{3}{2}})$ in both cases.

In figure 2(*b*, *c*) the distributions of the wall shear stress and the displacement thickness $A(x)$ are depicted. Again, comparison of the results for $\alpha = 5$ with calculations performed in I using a spectral method yields excellent agreement.

Finally, figure 3 shows a typical example of a comparison between the experimental data obtained by Leblanc & Ginoux (1970) in the 16 in. × 16 in. continuous supersonic wind tunnel of the von Kármán Institute and triple-deck solutions. The test conditions correspond to adiabatic flow over a flared cylinder with $\tilde{\alpha} = 7.5°$ at $M_\infty = 2.25$ with $Re = 8.7 \times 10^4$ and $a = 34.6$. Inspection of figure 3 indicates that the initial pressure rise in the interaction region is overpredicted by the asymptotic theory, as in the two-dimensional case studied by Rizzetta *et al.* (1978). Furthermore, it is seen that the pressure maximum is lower than the value determined experimentally by about 11 %. Again, as in the case of the flow over a compression ramp, Rizzetta *et al.* (1978), this discrepancy seems to be caused mainly by the linearization of the governing equations in the upper deck. For the above values of M_∞ and $\tilde{\alpha}$ linear theory underpredicts the pressure jump across the shock that forms at the corner by about 15 % if viscous effects are neglected. In contrast to the two-dimensional counterpart, however, viscous effects lead to a reduction of the pressure maximum in the axisymmetric case, which explains why the observed error is somewhat smaller than the estimate following from inviscid theory.

5. Results for negative cone angles

Numerical solutions of the full nonlinear interaction equations for $a = 1, \rho = 1$ and $0 < -\alpha \leqslant 7$ have been presented in I (figures 10 and 11). In all cases it was found that the pressure reaches a minimum value immediately downstream of the corner and then starts to rise again in agreement with the asymptotic relationship (8). As to be expected the pressure minimum is associated with a maximum of the wall shear stress (occurring slightly upstream of the corner) while the recompression of the flow leads to a minimum in the τ_w distribution downstream of $x = 0$. As pointed out in I the minimum value of τ_w decreases progressively with increasing values of $|\alpha|$ indicating the possibility of separation if $|\alpha|$ is sufficiently large. By extrapolation of the available data it was conjectured that incipient separation would occur at $\alpha \approx -11.2$.

Using the spectral method outlined in I additional calculations up to values of the turning angle of $\alpha = -12$ have subsequently been performed which showed the existence of separated regions for $\alpha < -11.18$ in good agreement with the extrapolated value. Unfortunately, however, no converged solution could be obtained for $\alpha < -12$. In order to study the flow properties at even smaller values of α the finite-difference method outlined in §3 was applied.

In figure 4 results for $\alpha = -11.5$ calculated by means of the spectral as well as the finite-difference method are compared. Owing to the inherently periodic nature of the spectral solution the ultimate decay of the pressure disturbances occurs faster than predicted by the asymptotic relationship which is in excellent agreement with the

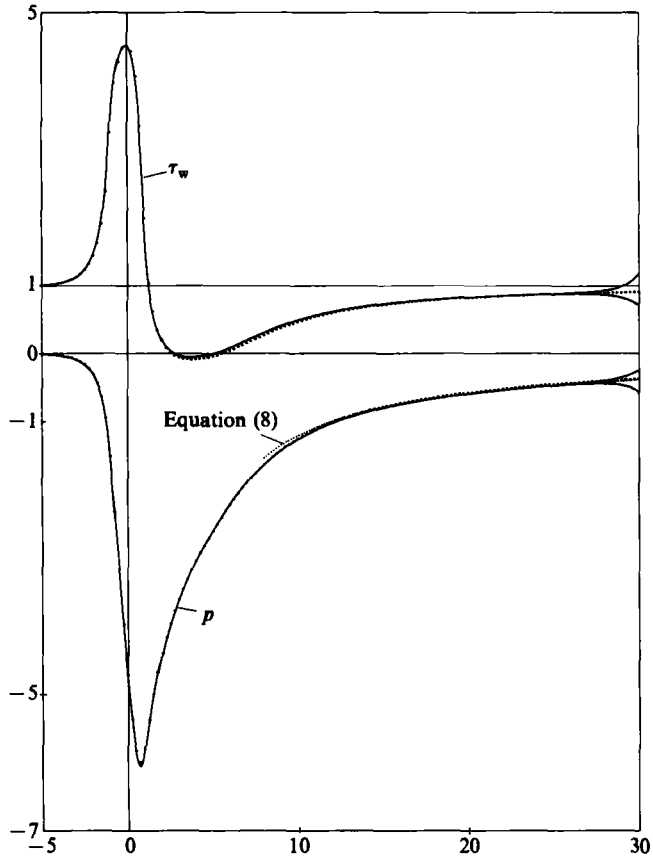

FIGURE 4. Numerical results for $a = 1$, $\rho = 1$ and $\alpha = -11.5$: ——, finite-difference method, $\Delta x = 0.05$, $\Delta z = 0.2$; · · · · · ·, spectral method, $N_x = 400$, $\Delta x = 0.25$, $N_z = 50$, $\Delta z = 0.3$.

pressure distribution following from the finite-difference scheme. The associated increase of the pressure gradient results in slightly smaller values of the shear stress inside and downstream of the separated-flow region.

Further decrease of α initially leads to solutions exhibiting separation bubbles of monotonically increasing length. However, efforts to extend the results beyond $\alpha = -11.5$ were hindered at first by an unexpected difficulty: even small changes of α resulted in shear-stress distributions with significantly longer regions of recirculating flow than before, indicating either the occurrence of a jump phenomenon or the existence of a range of ramp angles for which the solutions are no longer unique. Careful numerical studies indicate that the latter possibility is correct.

In figure 5 the positions of the separation point and the reattachment point are plotted as a function of α. If $\alpha > -11.28$ (A) the flow remains attached and the solutions are unique. In contrast, two solutions exhibiting relatively long recirculation zones and a third one yielding attached flow are obtained if $-11.42 < \alpha < -11.28$ (B). If the value of α decreases below -11.42 attached flow is no longer possible but the occurrence of three different types of separated flow is observed within the range $-12.42 < \alpha < -11.42$ (C). Unfortunately, the numerical scheme used in this study did not yield converged solutions with long separation bubbles for values of α less than -11.7. The numerical difficulties are most probably

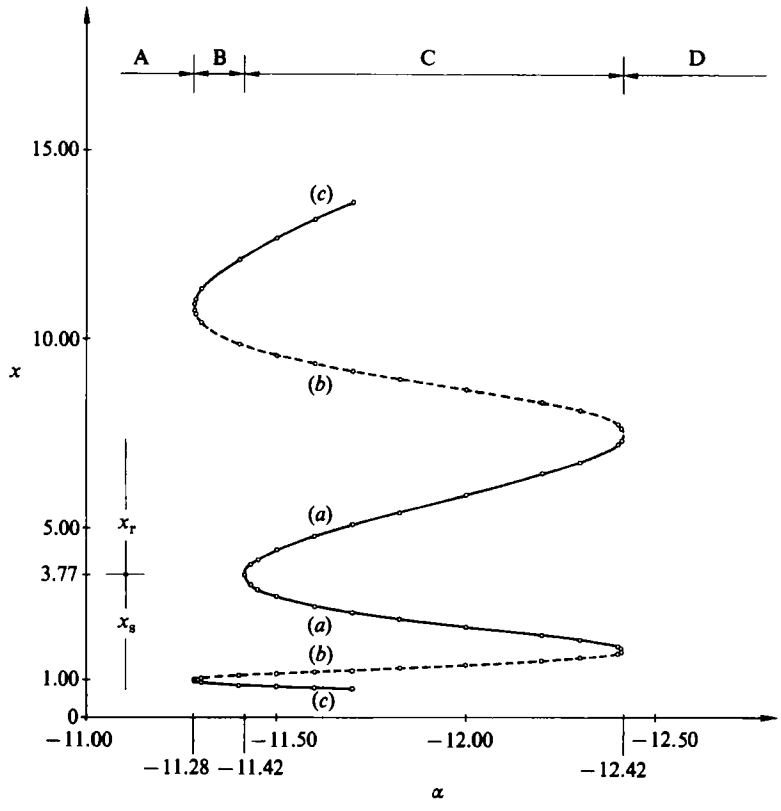

FIGURE 5. Position of the separation point x_s and the reattachment point x_r for various negative cone angles α ($a = 1, \rho = 1$).

associated with the rapid changes of the field quantities near the reattachment point which causes the FLARE approximation to break down. Based on the available numerical data, however, it seems reasonable to assume that the solutions are again unique if $\alpha < -12.42$ (D).

The distributions of the pressure, the wall shear stress and the displacement thickness for various values of α: $0 < -\alpha < 12.42$, and $\rho = 1$ are depicted in figure 6. To investigate whether the loss of uniqueness of triple-deck solutions for axisymmetric expansion ramps is caused by the smoothing of the corner, calculations for $\rho = 0$ have also been performed. It was found that the results are qualitatively similar to those for $\rho = 1$. As to be expected, incipient separation occurred at a smaller turning angle. Furthermore, the calculations showed that the range of values α for which triple-deck solutions were not unique (regions B and C) had reduced slightly in size.

As an example of the flow patterns that are obtained when α varies in region C, figure 7 shows streamlines in the lower deck for $\rho = 1, \alpha = -11.6$. A short and shallow separation bubble is barely visible in figure 7 (a), which corresponds to section (a) of the curve depicted in figure 5. The solution corresponding to section (b) (indicated by the dotted line) exhibits a longer separation bubble and separation occurs further upstream, figure 7 (b). Finally, the flow pattern associated with section (c) is plotted in figure 7 (c). The separation point has moved even further upstream and a long recirculation zone extends up to $x = 13.1$.

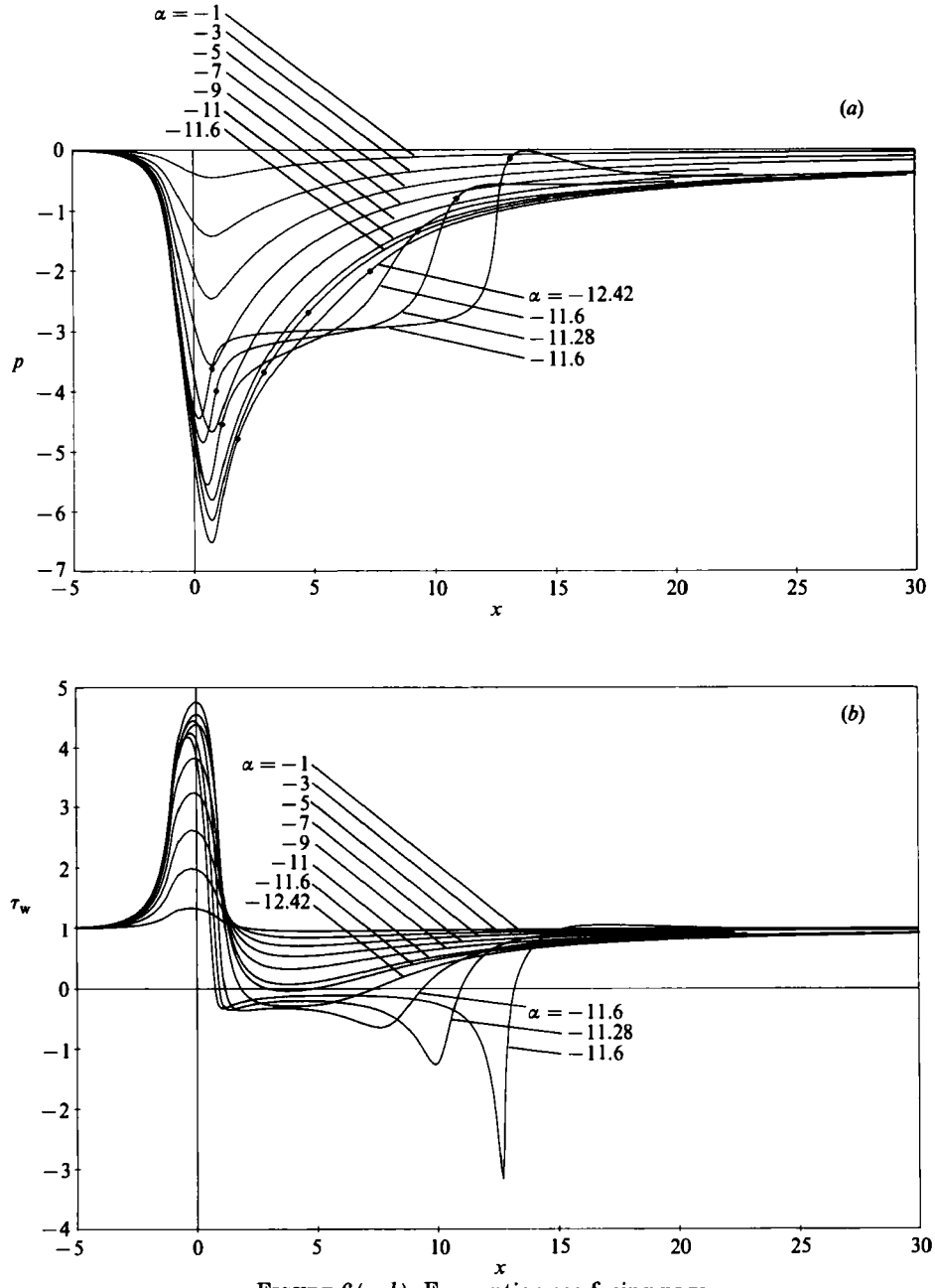

FIGURE 6(*a*, *b*). For caption see facing page.

The pressure and shear-stress distributions for $\rho = 1$ and $\alpha = -11.6$ are shown separately in figure 8 (*a*, *b*). The results for the solution with a short separation bubble (figure 7*a*) are qualitatively similar to those for attached flow plotted in figure 6. However, the two solutions with longer recirculation zones exhibit interesting new features. In particular, it is seen that the minimum of the pressure disturbances reduces as the length of the separated-flow region increases. More important, it is seen that the shape of the pressure and shear-stress distributions downstream of the

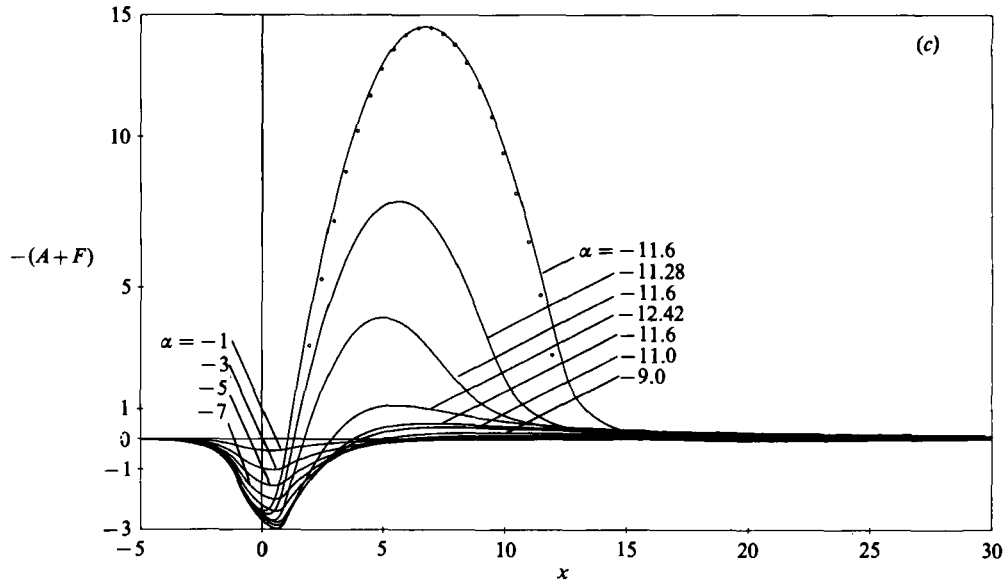

FIGURE 6. Numerical results for $a = 1, \rho = 1$ and various negative cone angles α: $\alpha = -1, -3, -5$: spectral method, $N_x = 400$, $\Delta x = 0.25$, $N_z = 50$, $\Delta z = 0.25$. Other values of α: finite-difference method, $\Delta x = 0.05$, $\Delta z = 0.4$. (*a*) Pressure distribution $p(x)$: $\diamond$, separation and reattachment points. (*b*) Wall-shear-stress distribution $\tau_w(x)$. (*c*) Displacement thickness distribution $-A(x)$: o, asymptotic relationship (9).

separation points now qualitatively resemble those for separated flows over axisymmetric compression ramps depicted in figure 2 (*a*) in spite of the fact that the pressure disturbances within the recirculation zones are negative. In fact, the occurrence of a region of almost constant negative pressure in the solution corresponding to the flow pattern in figure 7 (*c*) represents one of the most striking aspects of the present calculations. It should be noted, however, that the value of the plateau pressure is no longer only a function of the scaled cylinder radius a as in the case of axisymmetric compression ramps but will depend on the ramp angle α as well.

According to (5) changes of the free-stream Mach number and/or the Reynolds number result in changes of α even if the unscaled ramp angle $\tilde{\alpha}$ is held fixed. It is therefore interesting to investigate the associated variations of the flow properties. Let us assume then that α decreases continuously starting from a value within region A of figure 5 corresponding to attached flow. Incipient separation will occur at $\alpha = -11.42$ and a small separation bubble of continuously increasing length forms as one moves along branch (*a*) to even smaller values of α. However, when α exceeds the critical value of -12.42 solutions with a short separation bubble are no longer possible and consequently a discontinuous transition to solutions with a long recirculation zone corresponding to branch (*c*) must take place. If the process is reversed, that is if α increases again, the length of the separation bubble will initially decrease continuously until it assumes a minimum value at $\alpha = -11.28$. Further increase of α leads to a sudden disappearance of the recirculation zone and attached flow is recovered. The evolution of the flow pattern when α varies from A $\rightarrow$ D $\rightarrow$ A thus is characterized by the presence of a hysteresis.

Owing to the lack of numerical solutions and experimental data a complete picture of the flow structure for large values of $|\alpha|$ cannot be given yet. Guided by the available numerical results it seems reasonable to assume (i) that the separation point

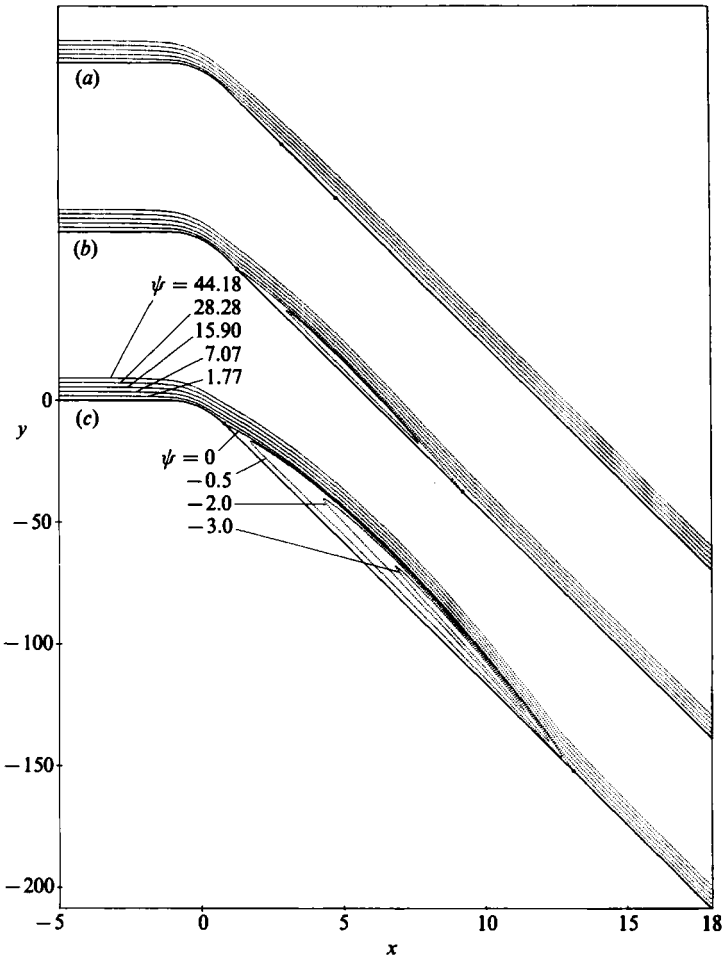

FIGURE 7. Streamlines in the lower-deck for $a = 1, \rho = 1$ and $\alpha = -11.6$ corresponding to the three different branches depicted in figure 5.

approaches the corner and (ii) that reattachment takes place over a distance which tends to zero on the triple-deck scale, both in the limit $|\alpha| \to \infty (\tilde{\alpha} \to 0, \epsilon \to 0, \tilde{\alpha}/\epsilon^2 \to -\infty)$.

As a consequence of (i) the shape of the free shear layer bounding the recirculation region should be described asymptotically by (9) far downstream of the corner. Thus, the distance L of the reattachment point from the corner can be estimated by calculating the intersection point between the free shear layer $y = A(x)$ and the wall $y = -\alpha x$. This leads to the relationship

$$p_0 \sim \frac{2a\alpha \ln L}{L}\left[1 - \frac{2}{\ln L}\left(\frac{3}{4} - \frac{1}{2}\ln\frac{2}{a}\right)\right] \tag{12}$$

between the almost constant (negative) pressure p_0 within the separated-flow region and the length L of the separation bubble.

According to (ii) the pressure rise associated with reattachment can be determined approximately from the equations for inviscid planar flow. Equating the pressure increase $\sim (-\alpha + A'(L))$ caused by the turning of the external flow and the pressure

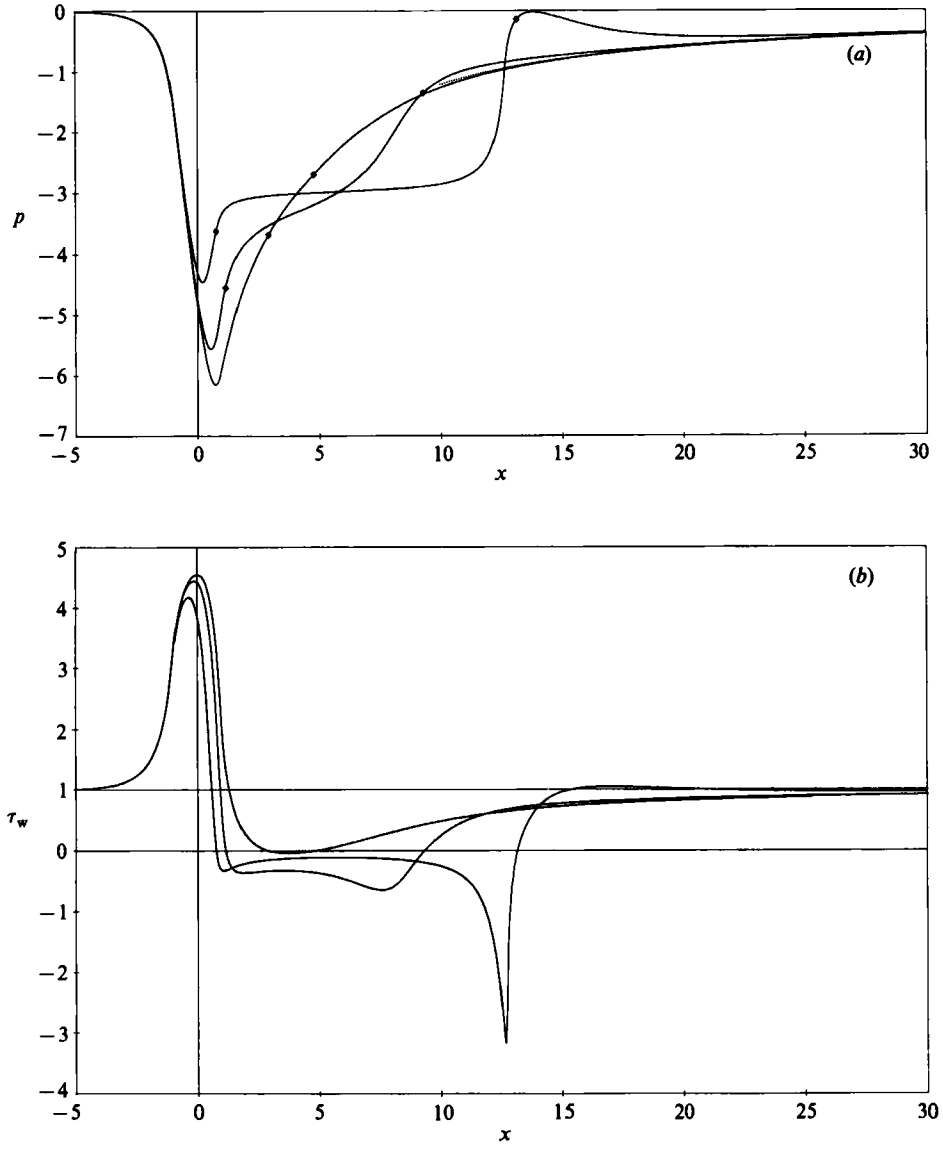

FIGURE 8. Pressure and wall-shear-stress distribution for $a = 1, \rho = 1$ and $\alpha = -11.6$ corresponding to the three different branches depicted in figure 5: ·····, asymptotic relationship (8); ◇, separation and reattachment points.

increase $\sim C^{-\frac{2}{3}}L^{\frac{2}{3}}$ generated by the isentropic compression along the reattachment streamline one obtains

$$\alpha - \frac{p_0 L}{a \ln L} \sim C^{-\frac{2}{3}}L^{\frac{2}{3}}. \tag{13}$$

Although this expression is analogous to (10), the resulting dependence of L on $|\alpha|$,

$$L \sim C|\alpha|^{\frac{3}{2}}, \tag{14}$$

is different from (11) holding for positive flare angles since $p_0 = O(\alpha \ln L/L)$ rather than $O(1)$ if $\alpha < 0$. Thus the length of the separated-flow region is much larger in the

latter case although the same mechanism of reattachment has been assumed for $\alpha > 0$ and $\alpha < 0$. Finally, it should be noted that (14) agrees with the relationship that determines the extent of the separation bubble generated by a compression ramp, Burggraf (1975).

Inspection of (9) and (12) indicates that the largest term neglected in the asymptotic relationship (14) is $O(|\alpha|^{\frac{3}{2}}/\ln|\alpha|)$. Consequently, the applicability of (14) is restricted to values α for which $1/\ln|\alpha| \ll 1$. Numerical solutions corresponding to branch (*c*) of figure 5, however, could be obtained for $\alpha > -11.7$, yielding $1/\ln|\alpha| > 0.4$ only. It is, therefore, not surprising that the predictions for L and p_0 which follow from (12) and (14) still differ significantly from the numerical results even for the largest value of the corner angle $\alpha = -11.7$. In this case evaluation of the asymptotic formulae (12) and (14) gives $L \approx 138.9, p_0 \approx -0.7$ while according to the numerical computations $L_n \approx 12.8, p_{0n} \approx -3.0$. For completeness rather than comfort it might be added that comparison between the numerical results of Rizzetta *et al.* (1978), Ruban (1978) and the asymptotic relationships derived by Burggraf (1975) for the flow over two-dimensional compression ramps leads to discrepancies of comparable magnitude.

Some encouragement may be gained, however, by checking (12) for consistency with the numerical results for L and p_0. For example, insertion of $L_n = 12.8$ into this asymptotic relationship yields $p_0 \approx -3.1$, which differs from $p_{0n} = -3.0$ by less than 4 %. Moreover, comparison of the asymptotic formula (9) with the numerical results for $\alpha = -11.6$ shows reasonably good agreement if a coordinate shift is allowed for, figure 6(*c*). The slope of the free shear layer near the reattachment point is overpredicted by about 10 %: $A'(12) \approx 17.4, A'_n\,(12) \approx 15.7$. In contrast, the corresponding values of the turning angle of the external flow, which follow by subtraction of two large numbers: $\Delta\alpha = A' + \alpha$, are 5.7 and 3.0, respectively, and differ by almost 100 %. This indicates that the large discrepancies between the asymptotic and numerical results for L and p_0 are mainly caused by the poor approximation of the turning angle of the external flow (left-hand side of (13)) due to the slow decay of logarithmic terms. Despite this difficulty, the above considerations seem to lend at least partial support to the proposed model which leads to (12) and (14). However, clearly much more analytical and numerical efforts will be necessary to produce a self-consistent and complete picture of the reattachment process.

6. Conclusions

Laminar supersonic flows past flared cylinders have been investigated in the limit of large Reynolds numbers for positive as well as negative cone angles α.

In the case of $\alpha > 0$ it is found that the axisymmetric spreading of the flow leads to an increase of the turning angle for incipient separation. If α is sufficiently large a plateau region, qualitatively similar to that observed for two-dimensional flows, is seen to develop upstream of the corner.

In contrast to the two-dimensional case, however, it is shown that large turning angles will also lead to separation if $\alpha < 0$. Moreover, the numerical results indicate that there exists a regime of turning angles in which the solution is not unique. In fact within this regime the flow structure may assume three different forms: (i) one with a short separation bubble the length of which decreases as $|\alpha|$ decreases; (ii) one with a longer separation bubble the length of which decreases as $|\alpha|$ increases; and (iii) one with a large separated-flow region having almost constant pressure, the length of which again increases with increasing values of $|\alpha|$. It does not seem to be

unlikely that it is this third form of solutions that describes the initial stages of the transition from attached flow ($\alpha > -11.42$) to grossly detached flow of Kirchhoff type as $|\alpha|$ increases beyond the value $|\alpha| = 12.42$. This leads to the conjecture that this transition is not a smooth process but is accompanied by a jump phenomenon. Non-uniqueness of interaction solutions has also been encountered in recent studies of marginally separated flows (Stewartson *et al.* 1982; Brown & Stewartson 1983). In this case the results form two branches as Γ (a suitably scaled angle of attack α) varies between 0 and 2.46 (with the exception of the range $1.25 < \Gamma < 1.40$ where four different solutions are possible) which are characterized by properties similar to those listed under (i) and (ii). In particular it is found that according to the second type of solution the point of flow reversal is tending to a limit while the reattachment point is tending to downstream infinity as $\Gamma \to 0+$, i.e. as the angle of attack is reduced to its value at incipient separation. However, as pointed out by one of the referees in Brown & Stewartson (1983): 'the scaling must break down at reattachment due to the promotion of neglected effects. He suggests that this trend may be reversed for a rescaled problem with the eddy growing as α increases and a match with grossly separated flows, such as the Kirchhoff free-streamline flow... eventually being achieved.'

It is of course tempting to assume that solution of type (iii) calculated in the present triple-deck study may be closely related to the branch of solutions (if it exists) that is missing in the description of marginal separation derived so far. It should, therefore, be interesting to investigate the properties of the classical boundary layer on smooth convex corners for large values of the scaled body radius a in more detail, to formulate the associated problem of marginal separation and to examine the behaviour of the solutions as a reduces to a quantity of order one.

As pointed out earlier, the differences between triple-deck solutions for planar and axisymmetric expansion ramps are mainly due to the effect of recompression which occurs in the latter case but is absent in supersonic two-dimensional flow. However, such a pressure increase downstream of the corner is present also in the two-dimensional case provided the external flow is subsonic and indeed the possibility of boundary-layer separation has been demonstrated by Smith & Merkin (1982). In view of the results obtained in the present investigation it seems well worth extending their calculations to even higher turning angles.

The authors are indebted to one of the referees for helpful comments. This research was sponsored by the 'Fonds zur Förderung der wissenschaftlichen Forschung in Österreich' under Contract P5557.

This paper is dedicated to Professor Dr K. Oswatitsch on the occasion of his 75th birthday.

REFERENCES

Brown, S. N. & Stewartson, K. 1983 On an integral equation of marginal separation. *SIAM J. Appl. Maths* **43**, 1119–1126.

Brown, S. N. & Williams, P. G. 1975 Self-induced separation. III. *J. Inst. Maths Applics* **16**, 175–191.

Burggraf, O. R. 1975 Asymptotic theory of separation and reattachment of a laminar boundary layer on a compression ramp. *AGARD paper* 168, Göttingen.

Daniels, P. G. 1974 Numerical and asymptotic solutions for the supersonic flow near the trailing edge of a flat plate at incidence. *J. Fluid Mech.* **63**, 641–656.

DANIELS, P. G. 1979 Laminar boundary-layer reattachment in supersonic flow. *J. Fluid Mech.* **90**, 289–303.

DANIELS, P. G. 1980 Laminar boundary-layer reattachment in supersonic flow. Part 2. Numerical solution. *J. Fluid Mech.* **97**, 129–144.

DUCK, P. 1984 The effect of a surface discontinuity on an axisymmetric boundary layer. *Q. J. Mech. Appl. Maths* **37**, 57–74.

DUCK, P. W. & BURGGRAF, O. R. 1986 Spectral solutions for three-dimensional triple-deck flow over surface topography. *J. Fluid Mech.* **162**, 1–22.

ERMAK, YU. N. 1969 Flow of a viscous incompressible fluid past the rounded leading edge of a slender airfoil. *Tr. TsAGI*, No. 1141.

GITTLER, PH. 1984 Laminare Wechselwirkungsvorgänge am schiebenden Flügel bei Überschallströmung. *Z. angew. Math. Mech.* **64**, T198–200.

GITTLER, PH. 1985 Dreidimensionale Wechselwirkungsvorgänge bei laminaren Grenzschichten. Dissertation, Technische Universität Wien.

HORTON, H. P. 1971 Adiabatic laminar boundary-layer/shock-wave interactions on flared axisymmetric bodies. *AIAA J.* **9**, 2141–2148.

KLUWICK, A. 1987 Interacting boundary layers. *Z. angew. Math. Mech.* **67**, T3–13.

KLUWICK, A., GITTLER, PH. & BODONYI, R. J. 1984 Viscous–inviscid interactions on axisymmetric bodies of revolution in supersonic flow. *J. Fluid Mech.* **140**, 281–301.

KLUWICK, A., GITTLER, PH. & BODONYI, R. J. 1985 Freely interacting axisymmetric boundary layers on bodies of revolution. *Q. J. Mech. Appl. Maths* **38**, 575–588.

LEBLANC, R. & GINOUX, J. 1970 Influence of cross flow on two dimensional separation. *Von Karman Institute for Fluid Dynamics, TN* 62.

LIGHTHILL, M. J. 1945 Supersonic flow past bodies of revolution. *Aero. Res. Counc. R & M* 2003.

MATVEEVA, N. S. & NEILAND, V. I. 1967 Laminar boundary layer near a corner point of a body. *Izv. Akad. Nauk SSSR, Mekh. Zhid. i Gaza*, **4**, 64–70.

MESSITER, A. F., HOUGH, G. R. & FEO, A. 1973 Base pressure in laminar supersonic flow. *J. Fluid Mech.* **60**, 605–624.

OSWATITSCH, K. 1958 Die Ablösebedingungen von Grenzschichten. In *Grenzschichtforschung* (ed. H. Görtler), IUTAM Symposium, Freiburg 1957, 1958, pp. 357–367. Springer.

REYHNER, T. A. & FLÜGGE-LOTZ, I. 1968 The interaction of a shock wave with a laminar boundary layer. *Intl J. Nonlinear Mech.* **3**, 173.

RIZZETTA, D., BURGGRAF, O. & JENSON, R. 1978 Triple-deck solutions for viscous supersonic and hypersonic flow past corners. *J. Fluid Mech.* **89**, 535–552.

ROSENHEAD, L. 1963 *Laminar Boundary Layers*. Oxford University Press.

RUBAN, A. I. 1978 *Izv. Akad. Nauk SSSR, J. Num. Math. & Math. Phys.* **18**, 1253–1265.

RUBAN, A. I. 1981*a* Asymptotic theory of short separation regions on the leading edge of a slender airfoil. *Izv. Akad. Nauk SSSR, Mekh. Zhid. i Gaza* **1**, 42–51.

RUBAN, A. I. 1981*b* Singular solutions of the boundary layer equations which can be extended continuously through the point of zero surface friction. *Izv. Akad. Nauk SSSR, Mekh. Zhid. i Gaza* **6**, 42–52.

SMITH, F. T. 1977 The laminar separation of an incompressible fluid streaming past a smooth surface. *Proc. R. Soc. Lond.* A **356**, 443–463.

SMITH, F. T. & MERKIN, J. H. 1982 Triple-deck solutions for subsonic flow past humps, steps, concave or convex corners, and wedged trailing edges. *Comput. Fluids* **10**, 7–25.

SMITH, F. T., SYKES, R. I. & BRIGHTON, P. W. M. 1977 A two-dimensional boundary layer encountering a three-dimensional hump. *J. Fluid Mech.* **83**, 163–176.

STEWARTSON, K. 1970*a* Is the singularity at separation removable? *J. Fluid Mech.* **44**, 347–364.

STEWARTSON, K. 1970*b* On laminar boundary layers near corners. *Q. J. Mech. Appl. Maths* **23**, 137–152 and corrections and addition **24** (1971), 387–389.

STEWARTSON, K., SMITH, F. T. & KAUPS, K. 1982 Marginal separation. *Stud. Appl. Math.* **67**, 45–61.

STEWARTSON, K. & WILLIAMS, P. G. 1973 Self induced separation. II. *Mathematika* **20**, 98–108.

SYKES, R. I. 1978 Stratification effects in boundary layer flow over hills. *Proc. R. Soc. Lond.* A **361**, 225–243.

SYKES, R. I. 1980 On three-dimensional boundary layer flow over surface irregularities. *Proc. R. Soc. Lond.* A **373**, 311–329.

VATSA, V. N. & WERLE, M. J. 1977 Quasi-three-dimensional laminar boundary-layer separations in supersonic flow. *Trans. ASME* I: *J. Fluids Engng* **99**, 634–639.

WARD, G. N. 1948 The approximate external and internal flow past a quasi-cylindrical tube moving at supersonic speeds. *Q. J. Mech. Appl. Maths* **1**, 225.

WERLE, M. J. & DAVIS, R. T. 1972 Incompressible laminar boundary layers on a parabola at angle of attack: a study of the separation point. *Trans. ASME* E: *J. Appl. Mech.* **20**, 7–12.

WERLE, M. J., VATSA, V. N. & BERTKE, S. D. 1973 Sweep effects on supersonic separated flows – a numerical study. *AIAA J.* **11**, 1763–1765.